Supplementary Material for:

High-Pressure Phase and Elasticity of Ammonia Hydrate

XINYANG LI[1], WEIGANG SHI[1], XIAODI LIU[2], ZHU MAO[1*]

[1]Laboratory of Seismology and Physics of Earth's Interior, School of Earth and Planetary Sciences, University of Science and Technology of China, Hefei, China

[2]Key Laboratory of Materials Physics, Institute of Solid State Physics, Chinese Academy of Sciences, Hefei, China

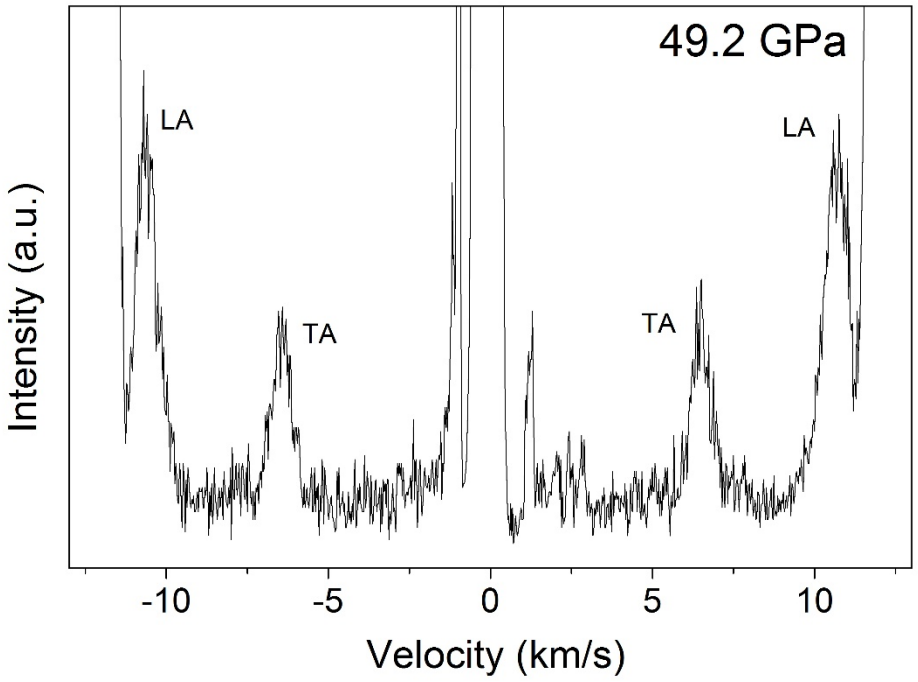

Figure S1. Representative Brillouin spectrum at 49.2 GPa and 300 K. LA: quasi-longitudinal mode; TA: quasi-transverse mode.

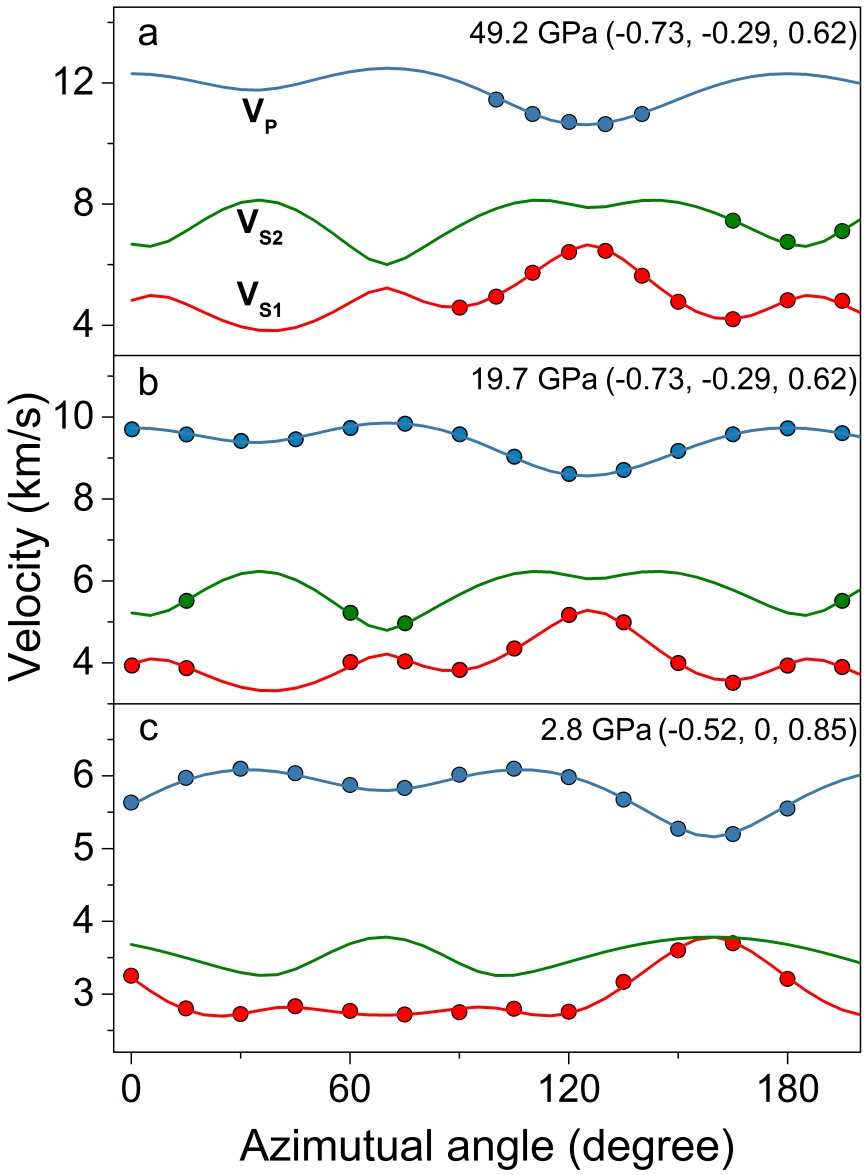

Figure S2. Acoustic velocities of ice-VII at high pressures. Blue: quasi-longitudinal velocity (V_P); green: fast quasi-shear velocity (V_{S2}); red: slow quasi-shear velocity (V_{S1}); solid lines: fitting results.

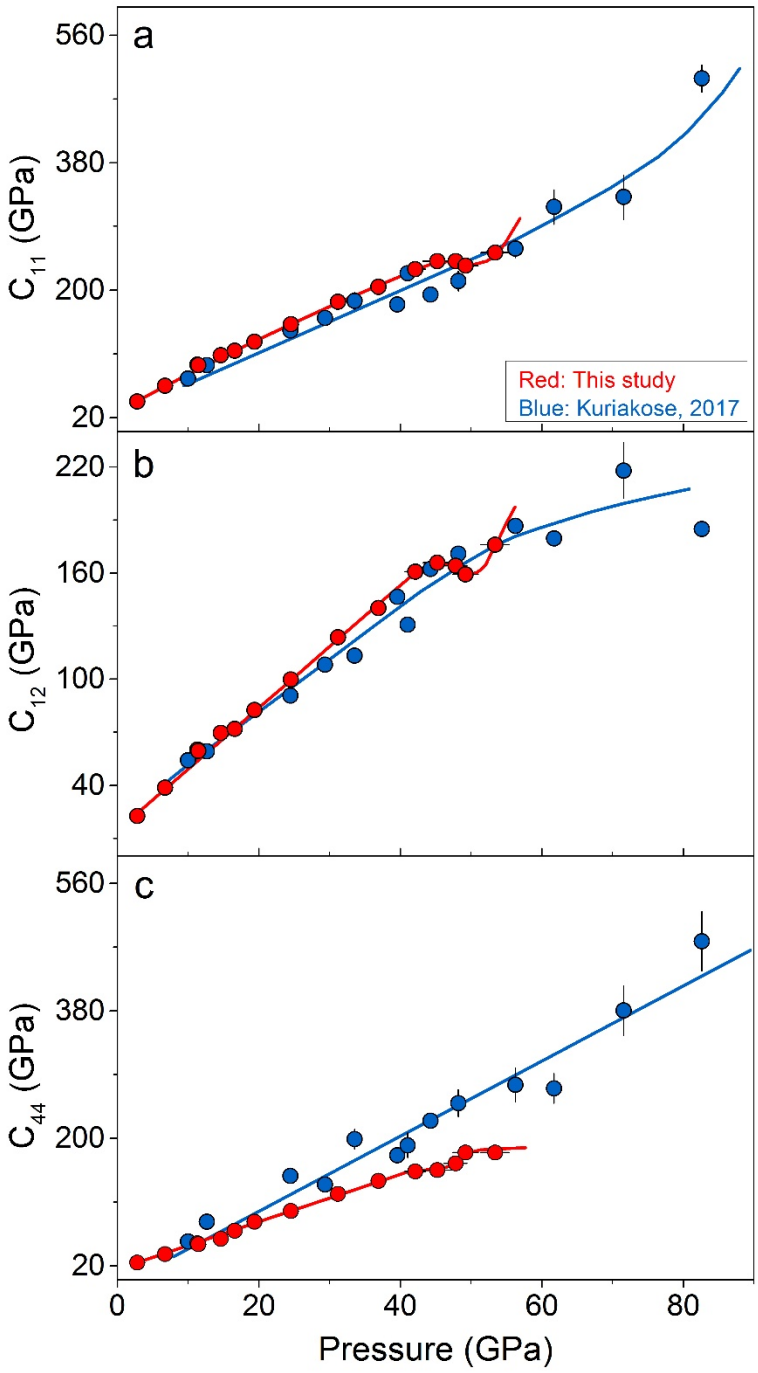

Figure S3. Single-crystal elasticity of ice-VII at high pressures and 300 K. Red: this study; blue: Kuriakose et al. (2017); lines: fitting results.

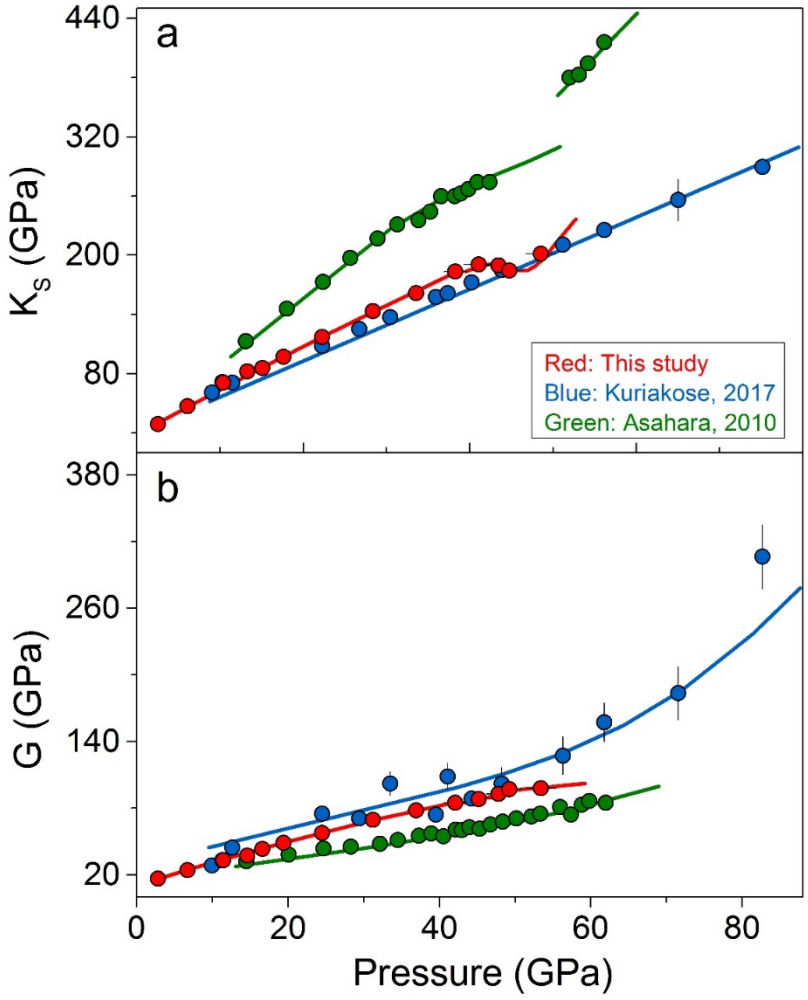

Figure S4. Bulk and shear moduli of ice-VII at high pressures and 300 K. Red: this study; blue: Kuriakose et al. (2017); green: Asahara et al. (2010); lines: fitting results.

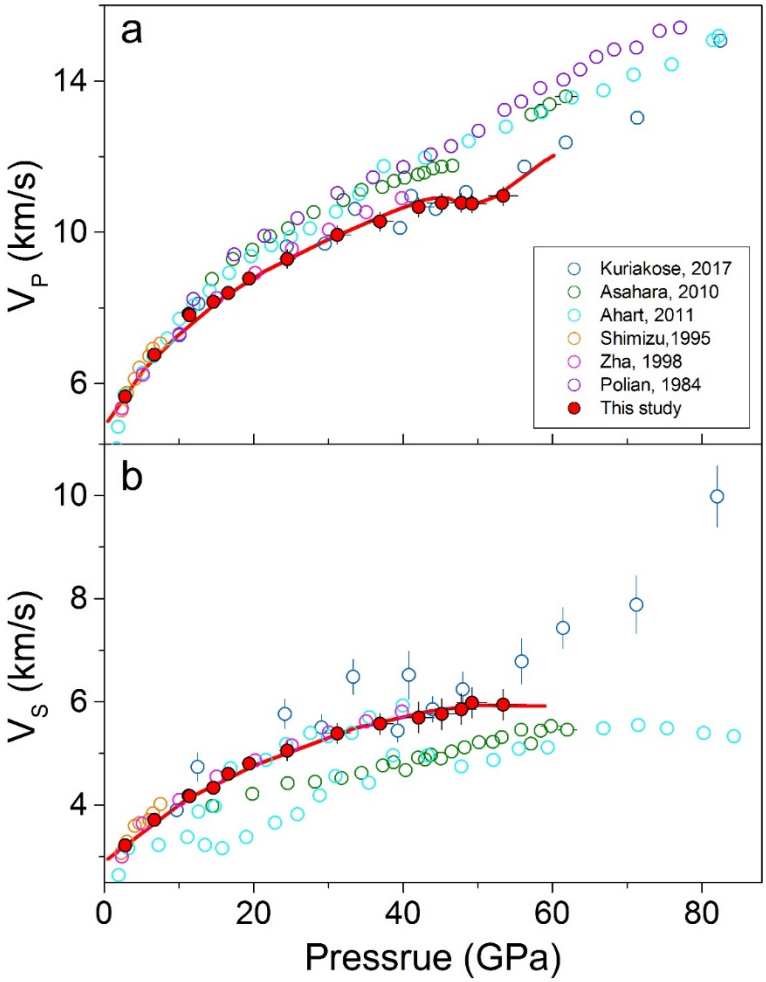

Figure S5. Sound velocity of ice-VII at high pressures and 300 K. Red: this study; blue: Kuriakose et al., 2017; green: Asahara et al., 2010; light blue: Ahart et al., 2011; orange: Shimizu et al., 1995; pink: Zha et al., 1998; purple: Polian et al., 1984; lines: fitting results.

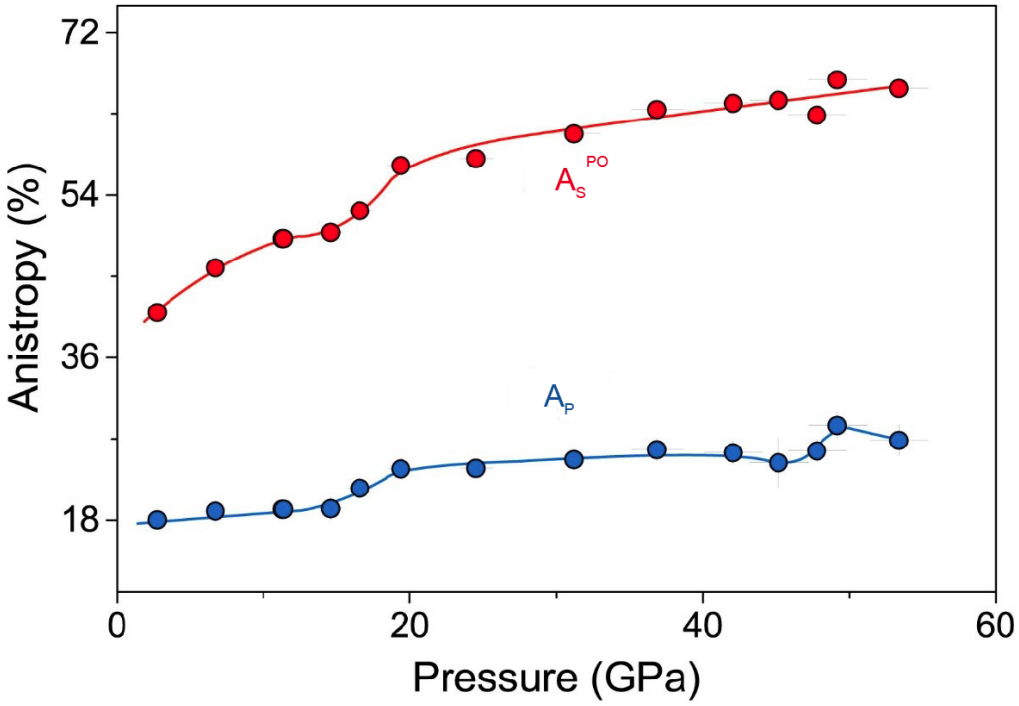

Figure S6. Velocity anisotropy of Ice-VII at high pressures and room temperatures. Blue: azimuthal compressional wave anisotropy; red: shear-wave splitting.

Table S1. Single-crystal elasticity of ice-VII at high pressures.

Phase	P (GPa)	Density* (g/cm^3)	C_{11} (GPa)	C_{44} (GPa)	C_{12} (GPa)	K_S (GPa)	G (GPa)
Ice-VII	2.7(3)	1.608	42.3(3)	23.9(3)	22.7(3)	29.2(3)	16.7(3)
	6.7(4)	1.740	64.8(6)	36.0(5)	38.6(6)	47.3(6)	24.0(5)
	11.4(4)	1.886	94.2(18)	50.2(13)	59.4(16)	71.0(14)	32.8(12)
	14.6(6)	1.980	107.7(30)	58.0(23)	69.6(29)	82.3(29)	37.2(22)
	16.6(8)	2.037	114.5(18)	68.9(13)	71.8(17)	86.0(17)	43.2(16)
	19.4(8)	2.114	127.2(18)	82.1(14)	82.6(14)	97.5(16)	48.9(15)
	24.5(9)	2.244	151.5(15)	97.3(10)	99.8(11)	117.1(13)	57.5(12)
	31.2(9)	2.398	183.5(19)	121.2(12)	123.7(14)	146.3(16)	69.7(12)
	36.9(11)	2.514	204.3(22)	139.9(17)	140.3(18)	161.6(20)	78.2(17)
	42.1(15)	2.606	229.1(38)	152.8(29)	160.7(32)	183.5(34)	84.6(30)
	45.2(20)	2.656	240.7(81)	155.0(76)	165.9(58)	190.9(78)	88.3(52)
	47.8(16)	2.694	240.9(54)	164.7(47)	164.2(53)	189.7(53)	92.6(51)
	49.2(18)	2.714	234.4(25)	179.8(18)	159.3(23)	184.3(24)	97.2(16)
	53.4(20)	2.767	252.8(43)	179.5(34)	176.0(38)	201.6(39)	97.9(32)

*Fitted from previous X-ray diffraction studies at high pressures (Loubeyre et al., 1999; Sugimura et al., 2008).